

Two-photon interference of photon pairs created in photonic crystal fibers

T. Nakanishi,^{1,2} K. Sakemi,¹ H. Kobayashi,¹ K. Sugiyama,^{1,2} and M. Kitano^{1,2}

¹Department of Electronic Science and Engineering, Kyoto University, Kyoto 615-8510, Japan

²CREST, Japan Science and Technology Agency, Tokyo 102-0075, Japan

(Dated: June 8, 2021)

We investigate a method to produce photon pairs by four-wave mixing in photonic crystal fibers (PCFs). By controlling the wavelength of the pump light, which determines the phase matching condition for four-wave mixing, we can obtain a broader spectrum of photon pairs than undesired Raman-scattered photons. We observe two-photon interference of photon pairs from a PCF with the help of an unbalanced Mach-Zehnder interferometer. Two-photon interference fringes with 83% visibility, which exceeds the classical limit of 50%, are obtained.

PACS numbers: 42.50.Dv, 42.50.St, 42.65.Lm, 03.65.Ud

I. INTRODUCTION

Photon pairs have been utilized in various fields such as fundamental physics and have found applications in quantum computation and communication, because they show various types of quantum correlations, for example, polarization correlation [1, 2], time-frequency correlation [3, 4], and spatial correlation [5]. Two-photon interference is one of the pure quantum phenomena attributed to quantum correlations. In experiments on two-photon interference, each photon pair behaves like a quantum object called a “*biphoton*,” whose effective energy (or frequency) is twice that of the original photons, and the interference fringe of the photon pair has half the period of a one-photon interference fringe [6]. Two-photon interference can be applied to high-resolution lithographic technology that overcomes the classical diffraction limit [7].

Three-wave mixing (TWM) in $\chi^{(2)}$ nonlinear crystals has been extensively used for the generation of photon pairs [2, 8]. Recently, four-wave mixing (FWM) in $\chi^{(3)}$ nonlinear material has also been studied as an effective method to produce entangled photon pairs [9, 10, 11, 12, 13, 14]. In TWM, a pump photon is split into a pair of photons, while in FWM, two photons in the pumping beam are converted into a pair of time-correlated photons. Therefore, in FWM, the resolution of two-photon interference is twice that of one-photon interference produced by the pumping light.

Optical fibers can be used for FWM because of the single-transverse-mode, low loss, propagation in the small cores. High-visibility interference requires a single-mode character that allows us to introduce the generated photon pairs into fiber-based networks easily. High nonlinearity can be achieved by confining the optical field to small area. Therefore, photonic crystal fibers (PCFs) with small core diameters are expected to be useful. The phase matching condition for FWM requires that the pump wavelength be close to the zero-dispersion wavelength of the fiber. Various types of PCFs with zero-dispersion wavelengths different from those of conventional fibers are commercially available.

In this paper, first, we discuss a method for the generation of photon pairs with a PCF. We derive the phase matching condition, which is a function of the dispersion relation of a $\chi^{(3)}$ medium, and obtain the photon pair spectrum from the

group velocity dispersion (GVD) in the datasheet of the PCF used in our experiment. The calculated result shows that the width of the photon pair spectrum is sufficiently high to evade the effect of Raman-scattered photons when the wavelength of pump light is slightly above the zero-dispersion wavelength. In accordance with the result, we demonstrate the generation of photon pairs and obtain 660 nm / 900 nm photon pairs at a rate of 2,000 counts/s and a pump power of 4 mW. Next, we introduce these photon pairs into an unbalanced Mach-Zehnder interferometer with a long arm and a short arm to verify their time correlation. In this interferometer, which shares the same principle as Franson interferometer [3, 4], two quantum states corresponding to the case where both photons transverse the same arm contribute to the two-photon interference. By precise coincidence counting for eliminating the possibility that each photon follows a different path, we obtain definite two-photon interference fringes with 83% visibility exceeding the classical limit, which provides clear evidence for the time correlation of the photon pairs.

II. GENERATION OF PHOTON PAIRS

In $\chi^{(3)}$ media, two pump photons are converted into a pair of photons, where one of them is called a signal photon and the other is called an idler photon, through spontaneous four-wave mixing. The energy conservation law requires that

$$2\omega_p = \omega_s + \omega_i, \quad (1)$$

where ω_p , ω_s , and ω_i correspond to the angular frequencies of the pump, signal, and idler photons, respectively. The spectrum of photon pairs is determined by the dispersion relation $k(\omega)$ of the medium. The number of photon pairs within a spectral width $\Delta\Omega$ and a time interval Δt is expressed as follows:

$$N = (\gamma PL)^2 \left| \frac{\sin(\kappa L)}{\kappa L} \right|^2 \Delta\Omega \Delta t, \quad (2)$$

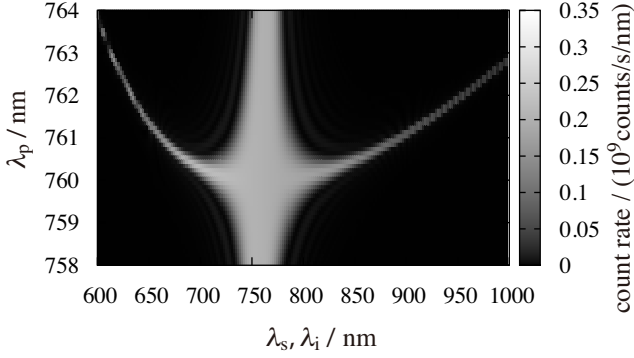


FIG. 1: Calculated spectrum of the photon pair (λ_s, λ_i) as a function of the pump wavelength λ_p . $P = 100$ mW.

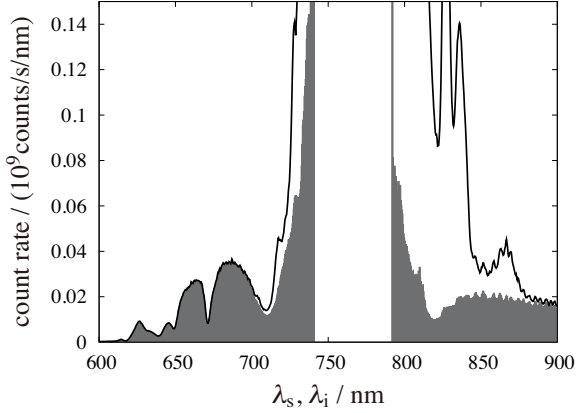


FIG. 2: The solid line represents the output spectrum from the PCF for $\lambda_p = 760.4$ nm and $P = 100$ mW. (The spectrum from 740 nm to 790 nm is not displayed.) The gray region represents the estimated spectrum of the photon pairs.

with

$$\kappa = \sqrt{\frac{\Delta k}{2} \left(\frac{\Delta k}{2} + 2\gamma P \right)}, \quad (3)$$

$$\Delta k = k(\omega_s) + k(\omega_i) - 2k(\omega_p), \quad (4)$$

where γ is a nonlinear coefficient, P is the pump power, and L is the interaction length [15].

Equation (1) shows that ω_s and ω_i are symmetrically located with respect to ω_p . The spectral separation between the pump photon and the photon pairs can be written as $\omega_s = \omega_p + \Delta\omega$ and $\omega_i = \omega_p - \Delta\omega$. The separation $\Delta\omega$ should be large in order to evade spontaneous Raman scattering, whose spectrum spreads over several hundred nanometers around the pump wavelength.

We use a polarization-maintaining PCF with the zero-dispersion wavelength $\lambda_0 = 760$ nm (Crystal Fiber, NL-PM-760), $\gamma = 102$ / W/km, and $L = 1.93$ m. The dispersion relation $k(\omega)$ can be derived from the group velocity dispersion $D(\omega)$, which is provided by the manufacturer. We can derive the spectrum of the photon pair (λ_s, λ_i) from Eq. (2)

as a function of the pump wavelength λ_p , as shown in Fig. 1. The spectrum is characterized by two distinct parts: the trunk near λ_p and the branches bifurcating at λ_0 . These parts are classified with the phase matching condition $\kappa \sim 0$ defined in Eq. (3): $\Delta k/2 + 2\gamma P \sim 0$ for the trunk part and $\Delta k \sim 0$ for the branch part. Because the trunk part usually overlaps the spectrum of the Raman-scattered photons, it is difficult to single out the photon pairs. In contrast, the spectrum of the branch part is well separated from that of the Raman-scattered photons for $\lambda_p \gtrsim \lambda_0$.

In order to avoid Raman scattering, we set the pump wavelength slightly higher than the zero-dispersion wavelength $\lambda_0 \sim 760$ nm. Figure 2 (solid line) shows an example of an output spectrum from the PCF for $\lambda_p = 760.4$ nm and $P = 100$ mW. The pump beam from a CW Ti:sapphire laser was coupled into the PCF, and the output spectrum was monitored by a spectrometer after passing it through a notch filter twice to eliminate the strong pump field. (The spectrum from 740 to 790 nm, which corresponds to the stop band of the notch filter, is not shown in Fig. 2.) The output spectrum (solid line) shows not only the photon pairs but also the Raman-scattered photons and residual pump photons. It is possible to estimate the fraction of the photon pairs from the fact that the generation rate of the photon pairs is proportional to P^2 , while that of the other photons is proportional to P . The gray region in Fig. 2 represents the estimated spectrum of the photon pairs. The result shows that although the Raman-scattered photons are distributed widely, the photon pairs dominate the spectrum below 720 nm and above 880 nm. We use $\lambda_s = 660$ nm and $\lambda_i = 900$ nm for the experiments on two-photon interference.

III. TWO-PHOTON INTERFERENCE OF PHOTON PAIRS FROM PCF

A. Two-photon interference in unbalanced Mach-Zehnder interferometer

For the experiment on two-photon interference, we use an unbalanced Mach-Zehnder interferometer comprising a long arm “L” with a length of L_L and a short arm “S” with a length of L_S as shown in Fig. 3. The photon pairs are fed to an input port P_0 , and they exit from one of the two output port P_1 and P_2 , after taking the long path or the short path.

We represent the photon state $|k_a, P_j\rangle$ with the wavenumber k_a ($a = s, i$) located at port P_j ($j = 0, 1, 2$). We calculate the state $|\Psi_1\rangle$ at which we observe the signal and idler photons exiting from the same output port P_1 :

$$|\Psi_1\rangle = \iint dk_s dk_i \Psi(k_s, k_i) |k_s, P_1\rangle |k_i, P_1\rangle, \quad (5)$$

where the spectrum $\Psi(k_s, k_i)$ is determined by the phase matching condition and the band-pass filters. The state $|k_a, P_1\rangle$ is a superposition of states in which the photon from P_0 follows either the short path S or the long path L :

$$|k_a, P_1\rangle = \frac{1}{\sqrt{2}} e^{ik_a L_L} |k_a, P_0\rangle + \frac{1}{\sqrt{2}} e^{ik_a L_S} |k_a, P_0\rangle. \quad (6)$$

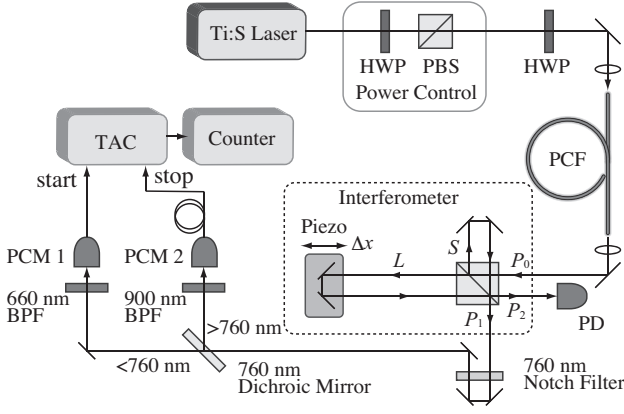


FIG. 3: Experimental setup for two-photon interference. HWP, half-wave plate; PBS, polarizing beam splitter; BPF, band-pass filter; PCM, photon counting module; TAC, time-to-amplitude converter.

Substituting Eq. (6) into Eq. (5), we obtain

$$|\Psi_1\rangle = \frac{1}{2} \iint dk_s dk_i \Psi(k_s, k_i) e^{i2k_p L S} (e^{i2k_p \Delta L} + e^{ik_s \Delta L} + e^{ik_i \Delta L} + 1) |k_s, P_0\rangle |k_i, P_0\rangle, \quad (7)$$

where we use the relation $k_s + k_i = 2k_p$ ($k_p = \omega_p/c$) derived from Eq. (1) and define $\Delta L = L_L - L_S$.

If the path difference ΔL is larger than the coherent length of each photon, the probability of finding both the photons at port P_1 is given as follows:

$$\langle \Psi_1 | \Psi_1 \rangle \propto 1 + \frac{1}{2} \cos(2k_p \Delta L). \quad (8)$$

The visibility of two-photon interference is only 50%, which is equal to the classical limit [16], because the second and third terms in Eq. (7) do not contribute to it. These terms correspond to the states where each photon follows a different path. Therefore, it is possible to eliminate them by counting only the photon pairs within a time interval shorter than the propagation time difference. In other words, we can postselect the first and fourth terms as follows:

$$|\Psi'_1\rangle = \frac{1}{2} \iint dk_s dk_i \Psi(k_s, k_i) e^{i2k_p L S} (e^{i2k_p \Delta L} + 1) |k_s, P_0\rangle |k_i, P_0\rangle. \quad (9)$$

Their probability is

$$\langle \Psi'_1 | \Psi'_1 \rangle \propto 1 + \cos(2k_p \Delta L). \quad (10)$$

All the terms in Eq. (9) contribute to the interference and produce the interference fringes with 100% visibility, which cannot be explained by the classical theory.

B. Experiments

A schematic representation of the experimental setup is shown in Fig. 3. The photon pairs from the PCF are sent

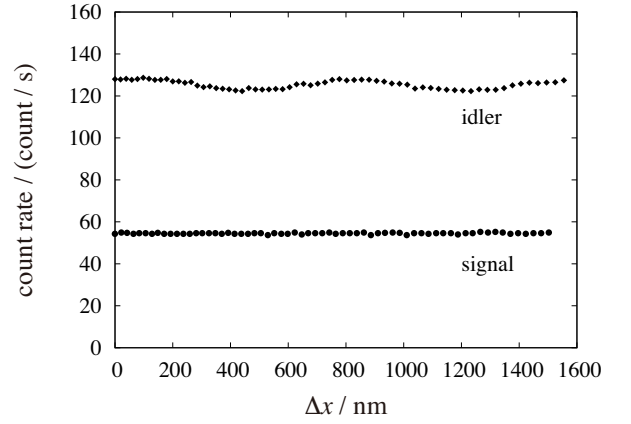


FIG. 4: One-photon interference of each photon. Circles (diamonds) represent the count rate of the signal (idler) photons as a function of Δx .

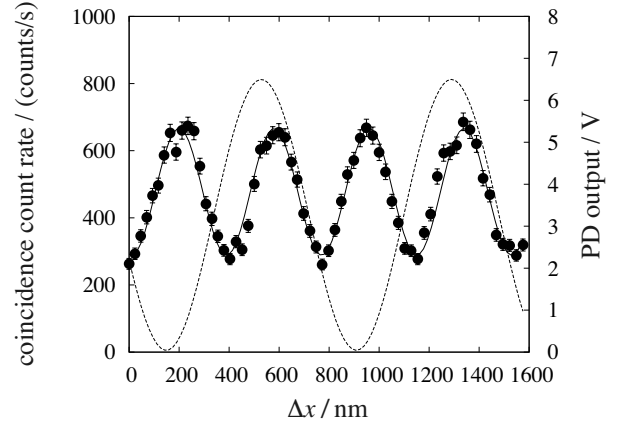


FIG. 5: The circles represent the coincidence count rates for $T = 6$ ns. The one-photon interference pattern of the pump light, which is detected by the PD, is superimposed for reference (dotted line).

to the unbalanced Mach-Zehnder interferometer. For elimination of the pumping light, the output light from P_1 is separated into two paths by a dichroic mirror after passing through a notch filter twice. The signal photon and the idler photon are detected by the respective photon counting modules, whose quantum efficiencies are 32% at 660 nm (PCM 1) and 33% at 900 nm (PCM 2). The band-pass filters with an FWHM of 10 nm passband are placed in front of the detectors. We use a time-to-amplitude converter (TAC) and an electronic counter for coincidence counting. The counter counts the number of photon pairs within a specific time interval T , which can be controlled by adjusting the discrimination levels of the counter.

We set the path difference $\Delta L \sim 60$ cm, which corresponds to the optical delay of $\tau = 2$ ns. The piezo actuator attached to one of the mirrors in the interferometer provides a variation of Δx in ΔL . We can derive the relation between Δx and the voltage applied to the piezo actuator from the one-photon

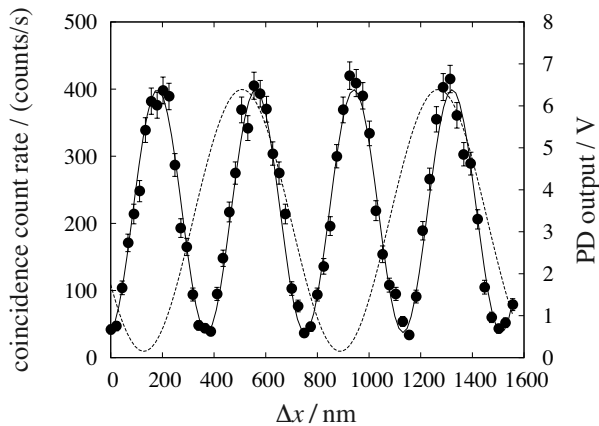


FIG. 6: The circles represent the coincidence count rates for $T = 1.5$ ns. The one-photon interference pattern of the pump light is superimposed for reference (dotted line).

interference pattern $\sin(k_p \Delta x)$ for the pump field by monitoring the signal of the photodiode (PD). In all experiments, the pump laser is operated at a power of 4 mW, which produces about 2,000 pairs per second at the detectors without the interferometer. The rate at which photon pairs are produced is sufficient for the experiment on two-photon interference, and the accidental coincidence rates are negligibly small.

We first measured one-photon interference for the signal and idler photons by individually counting the photons. Figure 4 shows the count rates as a function of Δx . As expected, there is no clear interference fringe, because ΔL is much larger than the coherent length of each photon. (The faint fringe for the idler photons can be attributed to the influence of the residual pump light.)

We performed two types of two-photon interference experiments by changing the gate time T for coincidence counting. First, we set $T = 6$ ns ($> \tau$) to measure the coincidence count rate that involves all the photon pairs passing through the interferometer. Figure 5 shows the one-photon interference pattern of the pump light (dotted line) for a reference and the two-photon interference pattern of the photon pairs (circles). The period of the two-photon interference fringe is half that of the one-photon interference fringe for the pump light. The visibility is only 40%, which is consistent with Eq. (8). Next, we set $T = 1.5$ ns ($< \tau$) to eliminate the possibility of the signal and idler photons following different paths. The results are shown in Fig. 6. We observed a two-photon interference fringe with 83% visibility, which exceeds the classical limit of

50%. The result shows that the photon pairs generated in the PCF have time correlations that can be explained only by the quantum theory. The main reason for the degradation of the visibility is mainly due to the chromatic aberration of the objective lens that collimates the photon pairs from the PCF. By using an objective lens specially designed for red and infrared wavelengths, the visibility of two-photon interference will be improved.

IV. CONCLUSION

In this paper, we report the generation of photon pairs by four-wave mixing in the photonic crystal fiber and the two-photon interference of the photon pairs. By maintaining the wavelength of the pump light slightly above the zero-dispersion wavelength, we obtained a wider spectrum of photon pairs as compared to that of Raman-scattered photons. We set the pump light wavelength to 760.4 nm and obtained 660 nm/900 nm photon pairs at 2,000 count/s with a pump power of only 4 mW, which could be generated by a diode laser. Because the photon pairs were emitted in a single-transverse mode of the fiber, all of them contributed to the interference effectively without any spatial filtering. The high brightness of the photon pairs per mode is an advantage of the fiber-based sources over crystal-based sources.

For higher photon-pair flux, we can use an intense pulse laser with slight modification in the two-photon interferometer [17]. In general, the conversion efficiency increases with the fiber length. However, due to the losses, a fiber longer than the fiber attenuation length, which is about 86 m for our fiber with 50 dB/km losses, is of no use.

Two-photon interference achieved using the unbalanced Mach-Zehnder interferometer produced clear interference fringes with 83% visibility, which exceeds the classical limit. The period of the fringes was half that of the pump light wavelength, which is different from the case of two-photon interference where photon pairs were generated through TWM. This shows that two-photon interference of photon pairs through FWM can be beneficial to high-resolution lithographic technology and phase-sensitive interferometries.

Acknowledgements

This research is supported by the global COE program “Photonics and Electronics Science and Engineering,” at Kyoto University and a Grant-in-Aid for Young Scientists (B), No. 18740247, from the Japan Society for the Promotion of Science.

-
- [1] A. Aspect, J. Dalibard, and G. Roger: Phys. Rev. Lett. **49** (1982) 1804.
 [2] P. Kwiat, K. Mattle, H. Weinfurter, and A. Zeilinger: Phys. Rev. Lett. **75** (1995) 4337.
 [3] J. D. Franson: Phys. Rev. Lett. **62** (1989) 2205.
 [4] P. G. Kwiat, A. M. Steinberg, and R. Y. Chiao: Phys. Rev. A **47**

- (1993) R2472.
 [5] M. D’Angelo, Y.-H. Kim, S. P. Kulik, and Y. Shih: Phys. Rev. Lett. **92** (2004) 233601.
 [6] K. Edamatsu, R. Shimizu, and T. Itoh: Phys. Rev. Lett. **89** (2002) 213601.
 [7] A. N. Boto, P. Kok, D. S. Abrams, S. L. Braunstein, C. P.

- Williams, and J. P. Dowling: Phys. Rev. Lett. **85** (2000) 2733.
- [8] P. G. Kwiat, E. Waks, A. G. White, I. Appelbaum, and P. H. Eberhard: Phys. Rev. A **60** (1999) 773.
- [9] K. Edamatsu, G. Oohata, R. Shimizu, and T. Itoh: Nature **431** (2004) 167.
- [10] M. Fiorentino, P. Voss, J. Sharping, and P. Kumar: IEEE Photonics Technol. Lett. **14** (2002) 983.
- [11] X. Li, P. L. Voss, J. E. Sharping, and P. Kumar: Phys. Rev. Lett. **94** (2005) 53601.
- [12] J. Chen, X. Li, and P. Kumar: Phys. Rev. A **72** (2005) 33801.
- [13] J. G. Rarity, J. Fulconis, J. Duligall, W. J. Wadsworth, and P. S. J. Russell: Optics Exp. **13** (2005) 534.
- [14] J. Fulconis, O. Alibart, J. L. O'Brien, W. J. Wadsworth, and J. G. Rarity: Phys. Rev. Lett. **99** (2007) 120501.
- [15] L. J. Wang, C. K. Hong, and S. R. Friberg: J. Opt. B **3** (2001) 346.
- [16] K. Sanaka, K. Kawahara, and T. Kuga: Phys. Rev. Lett. **86** (2001) 5620.
- [17] J. Brendel, N. Gisin, W. Tittel, and H. Zbinden: Phys. Rev. Lett. **82** (1999) 2594.